Drastic influence of micro-alloying on Frank loop nature in Ni and Ni-based model alloys

Kan Ma, Brigitte Décamps, Anna Fraczkiewicz, Frédéric Prima, Marie Loyer-Prost

Materials Research Letters

ISSN: (Print) 2166-3831 (Online) Journal homepage: https://www.tandfonline.com/loi/tmrl20

Drastic influence of micro-alloying on Frank loop nature in Ni and Ni-based model alloys

Kan Ma, Brigitte Décamps, Anna Fraczkiewicz, Frédéric Prima & Marie Loyer-Prost

To cite this article: Kan Ma, Brigitte Décamps, Anna Fraczkiewicz, Frédéric Prima & Marie Loyer-Prost (2020) Drastic influence of micro-alloying on Frank loop nature in Ni and Ni-based model alloys, Materials Research Letters, 8:5, 201-207, DOI: 10.1080/21663831.2020.1741042

To link to this article: https://doi.org/10.1080/21663831.2020.1741042

Published online: 16 Mar 2020.

MATER. RES. LETT.
2020, VOL. 8, NO. 5, 201–207
https://doi.org/10.1080/21663831.2020.1741042

MATERIALS RESEARCH LETTERS
Taylor & Francis
Taylor & Francis Group

REPORT

Drastic influence of micro-alloying on Frank loop nature in Ni and Ni-based model alloys

Kan Ma[a,d], Brigitte Décamps[b], Anna Fraczkiewicz[c], Frédéric Prima[d] and Marie Loyer-Prost[a]

[a]Université Paris-Saclay, CEA, Service de Recherches de Métallurgie Physique, Gif-sur-Yvette, France; [b]Laboratoire de Physique des 2 infinis Irène Joliot-Curie (IJCLab), Université Paris-Saclay, Orsay, France; [c]Ecole Nationale Supérieure des Mines de Saint Etienne, Centre Sciences des Matériaux et des Structures (SMS), St Etienne, France; [d]Chimie ParisTech-CNRS, Institut de Recherche de Chimie Paris, PSL Research University, Paris, France

ABSTRACT

Nickel and its alloys are f.c.c. model materials to investigate the elementary mechanisms of radiation damage and solute effects. This paper focuses on the drastic influence of micro-alloying (0.4 wt.% Ti or Cr) on the nature of defects after ion irradiation. Ultra-high purity materials are used to avoid impurity effects. For the first time, (i) large stable intrinsic Frank loops are identified in nickel while in alloys extrinsic Frank loops are observed; (ii) an eradication mechanism of intrinsic Frank loops is clearly identified; (iii) the morphology of Frank loops is shown to be characteristic of their nature.

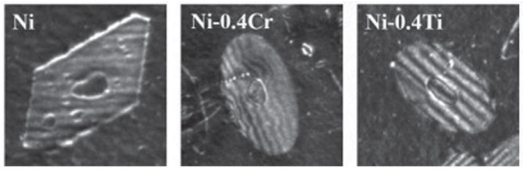

IMPACT STATEMENT

For the first time, a drastic influence of micro-alloying on the defect nature is shown in irradiated Ni systems. Minor addition of solutes modifies significantly elementary mechanisms of radiation damage.

ARTICLE HISTORY
Received 31 January 2020

KEYWORDS
Radiation damage; micro-alloying; Ni-based model alloys; Frank loop nature

1. Introduction

Advanced austenitic steels are candidate materials for current and future nuclear systems. Their main limitation is their macroscopic volume extension under irradiation, so-called void swelling [1,2]. Empirically, the fine-tuning of major elements (Ni, Cr) and the addition of some minor solutes (Ti, etc.) efficiently improved the swelling resistance [3]. To predict the structural evolution of these face-centered cubic (fcc) materials under irradiation, it is essential to understand the solute effects on the elementary mechanisms of radiation damage.

Model alloys such as pure nickel (Ni) and Ni-based binary alloys have been commonly used in the literature for this purpose [4–6]. In the early stage of irradiation, experiments in Ni showed a transition from stacking fault tetrahedra (SFT) dominated microstructure to a loop-dominated one [4]. Then, dislocation loops grow and produce line dislocation networks involved in the nucleation and growth of voids [7,8]. Meanwhile, the microstructure (density and size of dislocation loops and voids) is affected by the addition of solutes and impurities (like oxygen) over a wide range of metal materials (fcc, body-centered cubic (bcc)) and even novel concentrated solid solutions [9–16]. Thus, it can be seen that dislocation loops play an important role in the microstructural evolution in the early stage of irradiation. In Ni and its alloys, Frank partial dislocation loops (Burgers vector $1/3a_0 < 111 >$) and perfect loops (Burgers vector $1/2a_0 < 110 >$) were observed under neutron [5,6], electron [17–19] and ion [20–22] irradiation in a large range of temperatures (from 25 to 650°C). The nature of irradiation-induced Frank loops was identified as interstitial-type in most cases for all kinds of irradiation [6,17,18,20,22,23]. However, small metastable

CONTACT Marie Loyer-Prost marie.loyer-prost@cea.fr CEA Saclay, DES/ISAS/DMN/SRMP/JANNUS (Bât 126, pièce 58), PC. 162, 91191 Gif-sur-Yvette CEDEX, France

vacancy loops were claimed in irradiated nickel with electron [17] and ion [21,24].

To summarize the literature, the irradiated microstructure closely depends on solutes, the type of irradiations and is strongly affected by impurities. Furthermore, the nature of formed defects in nickel is not determined unambiguously. It has to be stressed that the existence of grown stable vacancy loops in nickel has not been proved and to the best of our knowledge the influence of solutes on the loop nature is unavailable in the literature. This paper focuses on a microstructural analysis of the early stage of ion irradiation in Ni and Ni-based model alloys. Ion irradiation is used in our study to reveal fundamentals of damage mechanisms. As micro-alloying (0.4 wt.% Ti) is efficient to reduce swelling [25], two alloys (Ni-0.4wt.%Ti and Ni-0.4wt.%Cr) are chosen and compared with Ni to understand the solute effect. As impurities affect the microstructure, ultra-high purity materials are elaborated. In this paper, the effects of micro-alloying with Cr or Ti on the nature of irradiation-induced defects are analyzed in detail and discussed.

2. Materials and methods

The ultra-high purity nickel (Ni) and the Ni-0.4wt.%Ti (Ni-Ti for short) with measured impurities (O, C, N, S) content in mass ppm respectively (3, 8, 2, 2 for Ni; 14, 2, 1, 4 for Ni-Ti), were manufactured by cold crucible induction melting at the Ecole des Mines de Saint Etienne (EMSE) in France. The high purity Ni-0.4wt.%Cr (Ni-Cr for short) was prepared also by induction melting in Service de Recherches Métallurgiques Physiques (SRMP) using pure chromium from J. Braconnot&Cie (> 99.996wt.%) and pure nickel from Goodfellow company (> 99.99wt.%). The raw materials were cut into 400 µm thick slides and then mechanically polished to 50-80 µm. 3 mm diameter disks were punched out and annealed at 1273 K for 2 h in a vacuum of 10^{-7} mbar followed by air-cooling. Annealed samples were perforated by twin-jet electro-polishing in a methanol-nitric acid solution for Transmission Electron Microscopy (TEM) observations. A low density of dislocations ($< 10^{10}$ m^{-2}) was measured by TEM in the initial state, before irradiation.

The irradiation was performed on the JANNuS-Saclay platform in CEA-Saclay. Thin foils were irradiated by 5 MeV Ni^{2+} ions at 450 ± 20 °C using a rastered beam. The temperature was monitored by 4 thermocouples respectively in contact with samples. The ion flux was $2.1 \pm 0.2 \times 10^{11}$ ions.cm^{-2}.s^{-1} and the fluence was $2.3 \pm 0.3 \times 10^{15}$ ions.cm^{-2}. The damage profile was calculated by the Stopping Range of Ions in Matter (SRIM) 2013 code [26] using Kinchin-Pease option with a displacement threshold energy of 40 eV. The final dose varied from 0.7 dpa near the surface to 2.2 dpa near the damage peak at depth of 1.5 µm.

After irradiation, TEM samples were lifted out far from thin zones using Focused Ion Beam (FIB) equipped on an FEI Helio 650 NanoLab dual-beam Scanning Electron Microscopy (SEM). The lifted out samples were then electro-polished using flash polishing technique to remove the FIB-induced defects [27]. The characterization of irradiation defects was performed using a 200 kV FEI TECNAI G2 TEM. Bright-Field (BF) mode and Weak-Beam Dark-Field (WBDF) mode were employed to optimize the defect contrast. All TEM micrographs were taken for $s_g > 0$. Dislocation loops were characterized under different two-beam conditions along several zone axes to apply the invisibility criterion for the analysis of the Burgers vector. The inside-outside method [28–30] was used to determine the nature of dislocation loops.

3. Results

In all materials, the microstructure is dominated by Frank loops and perfect loops. In FIB samples, loops are present from the irradiated surface to the depth of 1.5 µm. In pure Ni, all Frank loops are segmented. Very few voids are observed in Ni samples. In alloys, both loops and voids are present in FIB samples and the majority of Frank loops are not segmented. In both Ni and alloys, inner loops may be present within Frank loops. In Ni samples, no stacking fault is observed inside the inner loops whereas they are always observed in alloys (Figure 1 and Figure 2). The different morphology of Frank loops in Ni and the alloys raises questions about their nature. The determination of the nature of Frank loops was carried out. It is important to stress on that in each material, for tens of characterized loops, the same nature of almost all the defects was identified, independently on their Burgers vectors and geometric position (depth). In the following, the results of each material are presented for a representative loop, for which, detailed characterizations are given.

To demonstrate unambiguously the nature of a dislocation loop, (1) the Burgers vector, (2) the loop plane and (3) the inside-outside behavior in $\pm\mathbf{g}$ must be fully analyzed. For a pure edge loop, such as a Frank loop, (1) and (3) will be sufficient because the Burgers vector is perpendicular to the loop plane.

The analysis of the Burgers vector is carried out with the invisibility criterion [26]. It means that for a given two-beam condition with the diffraction vector $\mathbf{g}$, the dislocation loop with the Burgers vector $\mathbf{b}$ will be invisible or show a residual contrast if $|\mathbf{g} \cdot \mathbf{b}| = 0$. Figure 1(a-j)

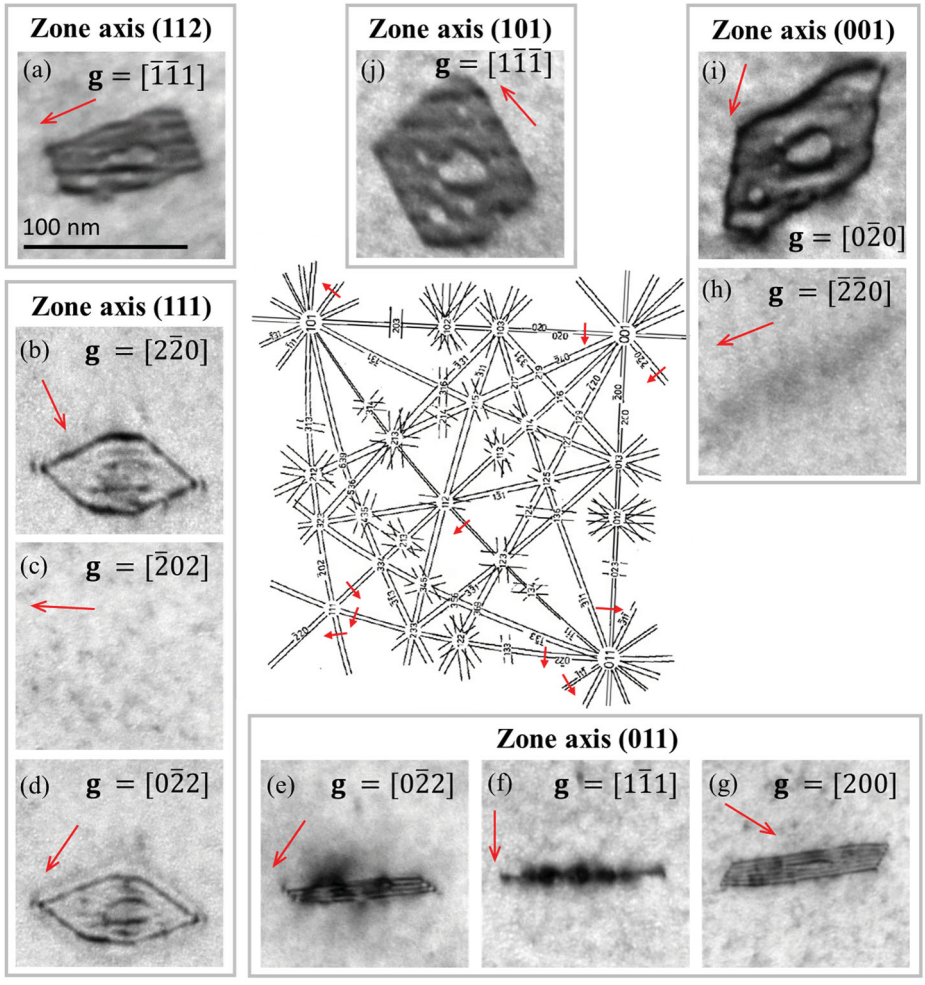

(k)

Table of visibility (V= visible, I= invisible)	Zone axes	[001]		[101]	[111]			[011]		[112]
	g / Possible b	0$\bar{2}$0	$\bar{2}\bar{2}$0	1$\bar{1}\bar{1}$	2$\bar{2}$0	$\bar{2}$02	0$\bar{2}$2	1$\bar{1}$1	200	$\bar{1}\bar{1}$1
	$\pm\frac{1}{3}$[111]	V	V	V	I	I	I	V	V	V
	$\pm\frac{1}{3}$[$\bar{1}$11]	V	I	V	V	V	I	V	V	V
	$\pm\frac{1}{3}$[1$\bar{1}$1]	V	I	V	V	I	V	V	V	V
	$\pm\frac{1}{3}$[11$\bar{1}$]	V	V	V	I	V	V	V	V	V

Figure 1. (a-j) Bright-field TEM images of irradiated Ni under ten two-beam conditions along different zone axis; central Kikuchi map is extracted from [28] and red arrows indicate the diffraction vector **g** in each micrograph with scale bar for all images indicated in (a); (k) table of visibility for both outer and inner loops based on **g**.**b** value.

presents the TEM micrographs of a dislocation loop in Ni with ten different **g** along different zone axes. The zone axis and diffraction vectors were cautiously indexed by comparing the Kikuchi lines and diffractions patterns with the reference schematic maps [28]. Since the loop is invisible for $\mathbf{g} = [\bar{2}02]$ (Figure 1(c)) and $\mathbf{g} = [\bar{2}\bar{2}0]$ (Figure 1(h)), it is a Frank loop with a Burgers vector of $\mathbf{b} = \pm a_0/3[1\bar{1}1]$. The visibility of the loop for the other **g** (Figure 1(k)) is in agreement with this Burgers vector.

For the inner small loops, their visibility is the same as the outer Frank loop for all the **g** analyzed. Thus, their Burgers vector is also $\pm a_0/3[1\bar{1}1]$. Figure 2(a) presents two Frank loops respectively in Ni-Cr and Ni-Ti. From their visibility (Figure 2(b)), both the outer Frank loop and the inner one have the same Burgers vector, $\mathbf{b} = \pm a_0/3[111]$ in Ni-Cr and $\pm a_0/3[1\bar{1}1]$ in Ni-Ti.

The sign of the Burgers vector depends on the nature of the loop. Figure 3 shows $\pm\mathbf{g}$ pairs of the three previous

(a)

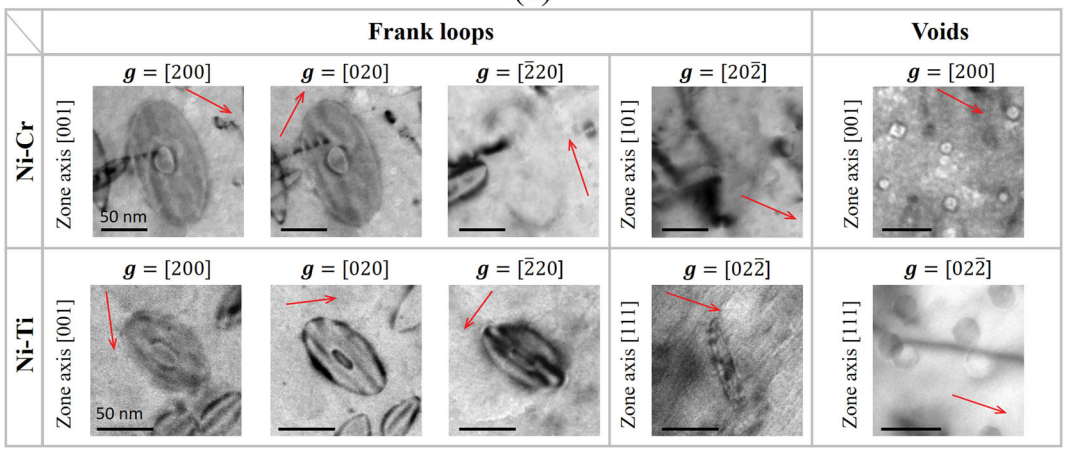

(b)

Table of visibility (V= visible, I= invisible)	Zone axes	[001]			[101]	[111]	BV analysis
	g / Possible b	200	020	$\bar{2}$20	20$\bar{2}$	02$\bar{2}$	
	$\pm\frac{1}{3}[111]$	V	V	I	I	I	Ni-Cr
	$\pm\frac{1}{3}[\bar{1}11]$	V	V	V	V	I	
	$\pm\frac{1}{3}[1\bar{1}1]$	V	V	V	I	V	Ni-Ti
	$\pm\frac{1}{3}[11\bar{1}]$	V	V	I	V	V	

Figure 2. (a) Bright-field TEM images of irradiated Ni-Cr and Ni-Ti (close to surface) under different two-beam conditions with diffraction vector **g** indicated by the red arrows with scale bar in each image denotes 50 nm; (b) table of visibility for both outer and inner loops.

Frank loops in Figure 1 and Figure 2. The inside-outside behavior of these loops is resumed in Table 1. In Ni, using the FS/RH convention [31] by considering the sense of the dislocation line as clockwise, the outside contrast of the outer loop for $\mathbf{g} = [020]$ gives $(\mathbf{g} \cdot \mathbf{b}) \cdot s_g > 0$. Thus, the Burgers vector of the outer Frank loop is $a_0/3[\bar{1}\bar{1}\bar{1}]$. Within the FS/RH convention, the Burgers vector points to the opposed direction against the loop plane normal $[1\bar{1}1]$, the outer Frank loop is therefore intrinsic (vacancy-type). On the contrary, the inner loops show a reverse contrast to the outer loop. The Burgers vector of inner loops is therefore $a_0/3[1\bar{1}1]$, corresponding to an extrinsic Frank loop (interstitial-type). No fault contrast is observed inside those inner loops in accordance with a perfect lattice. By the same analysis, the outer and inner loops are both of interstitial-type in Ni-Cr and Ni-Ti. As a contrast of the stacking fault is observed inside the inner loops, double layer extrinsic Frank loops are produced. Possible structures of these defects are given in Figure 3(p-r). Among all the studied loops, no Shockley partial was observed.

To sum up, intrinsic segmented single layer Frank loops are observed in irradiated Ni while extrinsic non-segmented (single and double layers) Frank loops are found in Ni-Cr and Ni-Ti. Only one intrinsic segmented Frank loop is detected in Ni-Cr. These results contrast with literature [17,21,24] which reports, in irradiated Ni, mostly extrinsic loops and sometimes small metastable vacancy loops. The different loop nature between Ni and its alloys together with the contrast behavior in Ni have to be understood.

4. Discussion

The drastic difference of the defect nature between Ni and micro-alloyed Ni is related to the behaviors of vacancies and interstitials. In Ni, vacancies form intrinsic Frank loops while, in the alloys, they form voids. Interstitials in Ni agglomerate as Frank loops nucleated in the middle of the intrinsic Frank loops eradicating the stacking fault. The growth of inner extrinsic Frank loops will lead to the total eradication of intrinsic Frank loops. Considering that loops in Ni are vacancy-type and partially eradicated, interstitials may be depleted in the damage production zone by migrating far away. Contrarily, interstitials in the alloys agglomerate as single or multi-layer Frank loops (two Frank loops in our case).

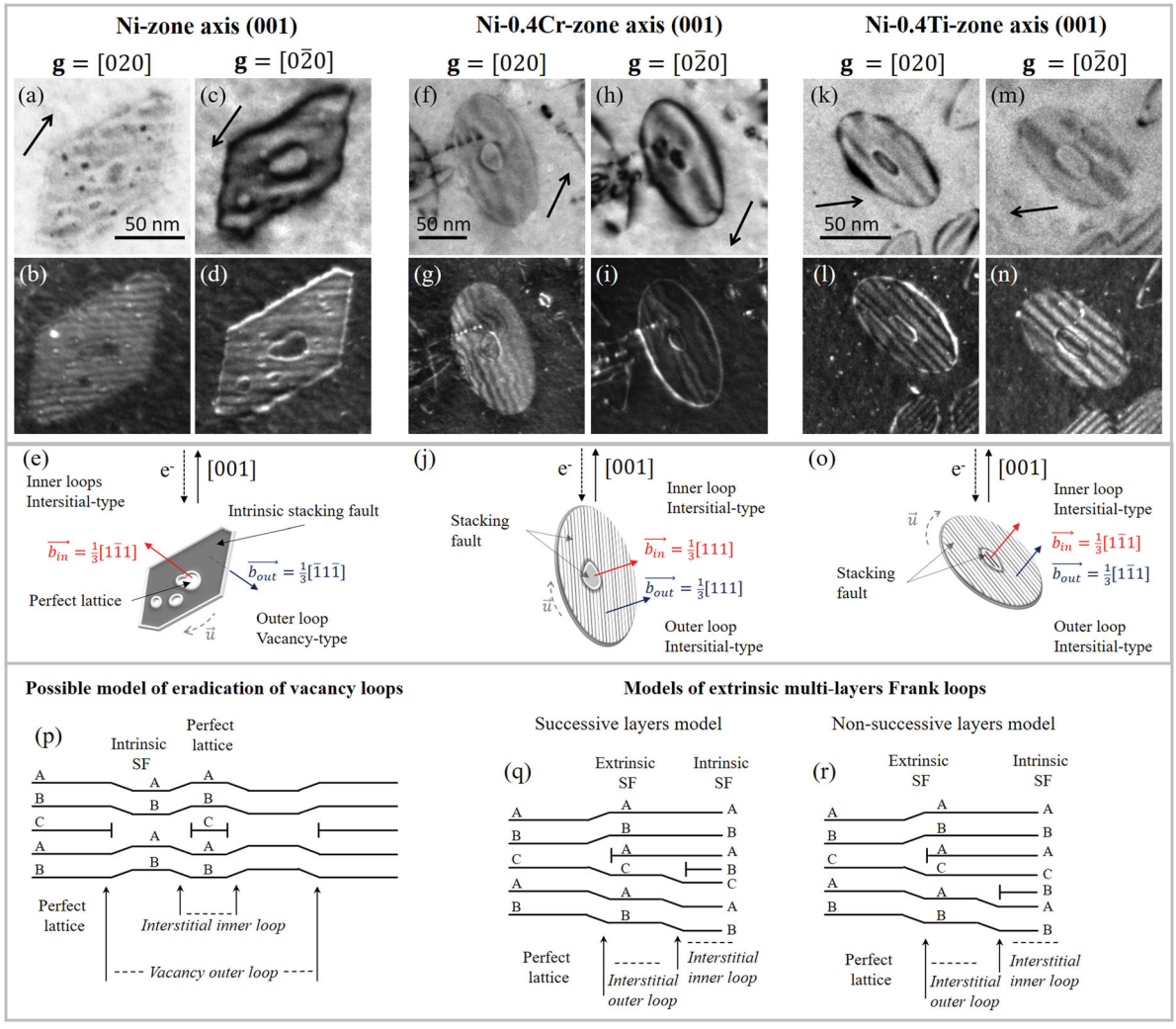

Figure 3. (a-o) Bright-field and corresponding weak-beam dark-field images for $\mathbf{g} = \pm[020]$ and the analysis of Frank loop nature in Ni (a-e); in Ni-Cr (f-j); in Ni-Ti (k-o); Scheme of Frank loop structure (p) in Ni and (q-r) two possible models in alloys suggested by [22].

Table 1. Inside-outside contrast and analysis of the nature of Frank loops in three materials.

			Contrast of loops				
Sample	Loop	**b** direction	$\mathbf{g} = [020]$	$-\mathbf{g} = [0\bar{2}0]$	$\mathbf{g} \cdot \mathbf{b}$ for **g**	b	Nature
Ni	Outer	$[1\bar{1}1]$	outside	inside	> 0	$a_0/3[\bar{1}1\bar{1}]$	vacancy
	Inner	$[1\bar{1}1]$	inside	outside	< 0	$a_0/3[1\bar{1}1]$	interstitial
Ni-Cr	Outer	[111]	outside	inside	> 0	$a_0/3[111]$	interstitial
	Inner	[111]	outside	inside	> 0		interstitial
Ni-Ti	Outer	$[1\bar{1}1]$	inside	outside	< 0	$a_0/3[1\bar{1}1]$	interstitial
	Inner	$[1\bar{1}1]$	inside	outside	< 0		interstitial

By molecular dynamics (MD) calculations, it was shown [13] that the low migration energy of interstitials and interstitial clusters (I-clusters) in Ni provokes their straight long-distance migration from the damage production region to the surface and deeper zones. On the contrary, as extrinsic Frank loops are observed in the alloys, interstitials may be trapped within the damage production region. Solutes like Fe and Co can increase the migration energy barrier of I-clusters, resulting in a short-distance complex migration trajectory [12]. Thus, interstitials atoms, I-clusters, and interstitial loops remain in irradiated zones leading to the growth of interstitial loops and the nucleation of a multi-layer structure as observed in our case. Such complex Frank loops were observed in irradiated nickel and alloys [22,32]. As the content of solute in our alloys is very low, a minor addition of Ti or Cr modifies drastically the migration of interstitials.

Meanwhile, the nucleation of vacancy defects occurs both in Ni (vacancy loops) and in the alloys (stable voids). Due to the much higher migration energy of vacancies compared to interstitials, the vacancy diffusion path is

quite short [12]. Thus, germs of vacancy loops created in cascades may absorb nearby free vacancies and grow in irradiated regions. It is interesting to wonder why vacancies agglomerate into different forms in Ni and in the alloys. In the literature, calculations in Ni demonstrate that if the surface energy of voids is reduced (presence of impurities like oxygen), voids may become the stable form instead of dislocation loops when the number of vacancies in the defect exceeds a critical value [13]. This critical value also depends on the stacking fault energy (SFE). In our case, we calculated the average number of vacancies present in loops for Ni ($\sim$20 nm in diameter $\approx 6 \times 10^3$ vacancies) and in voids for alloys ($\sim$10 nm in diameter $\approx 3 \times 10^4$ vacancies). In both cases, we found values lower than the critical value found in the reference [13], which explains our observations in Ni. Meanwhile, in the alloys, voids are the stable form, so they are energetically favored by the addition of Ti and Cr. It suggests an influence of a very small amount of solutes on the SFE and/or the surface energy of voids.

It has to be mentioned that the observation of stable grown vacancy Frank loops at different depths in our irradiated Ni samples seems to contrast with previous studies [17,21,24] where vacancy loops were only reported either near other dislocations or were metastable. This difference may be understood considering the type of irradiation (issue of vacancy loop nucleation with electrons and light ions) and the presence of impurities (oxygen and nitrogen) which is believed to affect the microstructure [13,22].

At last, it is worth noting that the morphology of Frank loops is found to depend drastically on its nature: segmented for intrinsic and not segmented for extrinsic. Even the only observed intrinsic Frank loop in the alloys is segmented. These segmented intrinsic Frank loops are similar to those obtained after quenching in nickel [33] and in quenched aluminium [34,35] which are assumed to be intrinsic.

5. Conclusions

Microstructural analysis was conducted in ultra-high purity Ni and micro-alloyed Ni (with Ti or Cr) irradiated by self-ion at high temperature. A drastic influence of micro-alloying on the nature of radiation-induced Frank loops is observed. In Ni, vacancies form intrinsic Frank loops. Interstitials agglomerate also as Frank loops but only inside existing intrinsic Frank loops and eradicate the stacking fault. In the alloys, vacancies form voids while interstitials agglomerate as single or multilayer extrinsic Frank loops. For the first time, (i) the real impact of micro-alloying on Frank loop nature and fine microstructure is shown; (ii) large stable intrinsic Frank loops are identified in nickel; (iii) an eradication mechanism of intrinsic Frank loops by inner extrinsic Frank loops is clearly shown; (iv) the morphology of Frank loops is shown to be a characteristic feature of their nature. These observations of fundamental properties of radiation-induced defects introduce new considerations in theoretical calculations, which will contribute significantly to a better understanding of the elementary mechanisms of radiation damage and solute effects in f.c.c. structure.

Acknowledgments

The research was supported by the NEEDS program (CNRS-CEA-EDF-ANDRA-AREVA-IRSN-BRGM), the RMATE project (CEA) and by the French government, managed by the French National Research Agency, under the 'Investissements d'avenir' program (No. ANR-11-EQPX-0020). Ion beam irradiation was performed by JANNuS-Saclay-CEA team; their support is gratefully acknowledged. Authors thank P. XIU and C. LU for their useful help on the flash polishing.

Disclosure statement

No potential conflict of interest was reported by the author(s).

References

[1] Lauritzen T, Withop A, Wolff UE. Swelling of austenitic stainless steels under fast neutron irradiation at elevated temperatures. Nucl Eng Des. 1969;9:265–268.
[2] Bates JF, Powell RW. Irradiation-induced swelling in commercial alloys. J Nucl Mater. 1981;102:200–213.
[3] Yvon P. Structural materials for Generation IV nuclear Reactors. 1st ed. Cambridge, United Kingdom: Woodhead Publishing; 2016.
[4] Zinkle SJ, Snead LL. Microstructure of copper and nickel irradiated with fission neutrons near 230°C. J Nucl Mater. 1995;225:123–131.
[5] Brimhall JL, Mastel B. Stability of voids in neutron irradiated nickel. J Nucl Mater. 1969;33:186–194.
[6] Yoshiie T, Xu Q, Satoh Y, et al. The effect of alloying elements on the defect structural evolution in neutron irradiated Ni alloys. J Nucl Mater. 2000;283-287:229–233.
[7] Garner FA. Radiation damage in austenitic steels. Comprehensive nuclear materials [Internet]. New York, United States of America: Elsevier; 2012.
[8] Stubbins JF, Garner FA. Swelling and microstructure of high purity nickel irradiated with fast neutrons in EBR-II. J Nucl Mater. 1992;191:1295–1299.
[9] Porollo SI, Dvoriashin AM, Konobeev YV, et al. Microstructure and swelling of neutron irradiated nickel and binary nickel alloys. J Nucl Mater. 2013;442:S809–S812.
[10] Watanabe H, Aoki A, Muroga T, et al. Effect of combined addition of phosphorus and titanium on microstructural evolution in Fe-Cr-Ni alloys. J Nucl Mater. 1991;179–181:529–533.
[11] Porollo S., Dvoriashin A., Vorobyev A., et al. The microstructure and tensile properties of Fe–Cr alloys after

neutron irradiation at 400°C to 5.5–7.1 dpa. J Nucl Mater. 1998;256:247–253.
[12] Lu C, Niu L, Chen N, et al. Enhancing radiation tolerance by controlling defect mobility and migration pathways in multicomponent single-phase alloys. Nat Commun. 2016;7:13564.
[13] Seitzman LE, Wang LM, Kulcinski GL, et al. The effect of oxygen on void stability in nickel and austenitic steel. J Nucl Mater. 1986;141–143:738–742.
[14] Singh BN, Leffers T, Makin MJ, et al. Effects of implanted helium on void nucleation during hvem irradiation of stainless steel containing silicon. J Nucl Mater. 1981;104:1041–1045.
[15] Bhattacharya A, Meslin E, Henry J, et al. Effect of chromium on void swelling in ion irradiated high purity Fe–Cr alloys. Acta Mater. 2016;108:241–251.
[16] Jin K, Lu C, Wang LM, et al. Effects of compositional complexity on the ion-irradiation induced swelling and hardening in Ni-containing equiatomic alloys. Scr Mater. 2016;119:65–70.
[17] Urban K. Growth of defect clusters in thin nickel foils during electron irradiation (I). Physica Status Solidi (a). 1971;4:761–772.
[18] Yoo MH, Stiegler JO. Growth kinetics and 'preference factor' of Frank loops in nickel during electron irradiation. Philos Mag. 1977;36:1305–1315.
[19] Norris DIR. Dislocation loop growth in an electron irradiated thin foil. Philos Mag. 1970;22:1273–1278.
[20] Pinizzotto RF, Chen LJ, Ardell AJ. Nickel and nitrogen ion irradiation induced void swelling and defect microstructures in Ni-Al, Ni-Cr and Ni-Ti solid solutions. Metall Trans A. 1978;9:1715–1727.
[21] Robinson TM, Jenkins ML. Heavy-ion irradiation of nickel and nickel alloys. Philos Mag A. 1981;43:999–1015.
[22] Chen LJ, Ardell AJ. The observation of multiple-layer loops in nickel base alloys under ion bombardment. Physica Status Solidi (a). 1976;34:679–690.
[23] Mazey DJ, Hudson JA. Observation of large faulted interstitial loops in proton-irradiated nickel. J Nucl Mater. 1970;37:13–17.
[24] Ishino S, Fukuya K, Muroga T, et al. In-situ microstructural observation of radiation damage in nickel produced by energetic heavy particles. Journal of Nuclear Materials. 1984;122&123:597–601.
[25] Gavoille P, Courcelle A, Seran JL, et al. Mechanical Properties of Cladding and Wrapper Materials for the ASTRID Fast-Reactor Project. International Atomic Energy Agency (IAEA): IAEA; 2013. p. v. Available from: http://inis.iaea.org/search/search.aspx?orig_q = RN:45089554.
[26] Ziegler JF. Nuclear instruments and methods in physics research section B: beam interactions with materials and atoms. SRIM-2003. 2004;219:1027–1036.
[27] Horváth B, Schäublin R, Dai Y. Flash electropolishing of TEM lamellas of irradiated tungsten. Nucl Instrum Methods Phys Res Sect B. 2019;449:29–34.
[28] Loretto MH, Smallman RE. Defect analysis in electron microscopy. London, United Kingdom: Chapman and Hall; 1975.
[29] Hirsch PB. Electron microscopy of thin crystals. Huntington, United States of America: Robert E. Krieger Publishing Company; 1967.
[30] Jenkins ML. Characterisation of radiation-damage microstructures by TEM. J Nucl Mater. 1994;216:124–156.
[31] Bilby BA, Bullough R, Edwin S. Continuous distributions of dislocations: a new application of the methods of non-Riemannian geometry. Proc. R. Soc. Lond. A. 1955;231:263–273.
[32] Das G, Mitchell TE. Irradiation damage of nickel in a high-voltage electron microscope. J Nucl Mater. 1975;56:297–306.
[33] Humble P, Loretto MH, Clarebrough LM. The nature of defects in quenched nickel. Philos Mag. 1967;15:297–303.
[34] Edington JW, Smallman RE. Faulted dislocation loops in quenched aluminium. The Philosophical Magazine: A Journal of Theoretical Experimental and Applied Physics. 1965;11:1109–1123.
[35] Eikum AK, Maher DM. Electron microscope image contrast from multiple Frank dislocation loops. Phys. Stat. Sol. (a). 1975;29:281–292.